
**Prediction intervals for overdispersed binomial
endpoints and their application to toxicological
historical control data**

Max Menssen^{1*}, Jonathan Rathjens²

*: Corresponding author

1: Department of Biostatistics, Leibniz University Hannover

2: Early Development Statistics, Chrestos Concept GmbH & Co. KG, Essen

Abstract

For toxicology studies, the validation of the concurrent control group by historical control data (HCD) has become requirements. This validation is usually done by historical control limits (HCL), which should cover the observations of the concurrent control with a predefined level of confidence. In many applications, HCL are applied to dichotomous data, e.g. the number of rats with a tumor vs. the number of rats without a tumor (carcinogenicity studies) or the number of cells with a micronucleus out of a total number of cells. Dichotomous HCD may be overdispersed and can be heavily right- (or left-) skewed, which is usually not taken into account in the practical applications of HCL.

To overcome this problem, four different prediction intervals (two frequentist, two Bayesian), that can be applied to such data, are proposed. Based on comprehensive Monte-Carlo simulations, the coverage probabilities of the proposed prediction intervals were compared to heuristical HCL typically used in daily toxicological routine (historical range, limits of the np-chart, $\text{mean} \pm 2 \text{SD}$). Our simulations reveal, that frequentist bootstrap calibrated prediction intervals control the type-1-error best, but, also prediction intervals calculated based on Bayesian generalized linear mixed models appear to be practically applicable. Contrary, all heuristics fail to control the type-1-error.

The application of HCL is demonstrated based on a real life data set containing historical controls from long-term carcinogenicity studies run on behalf of the U.S. National Toxicology Program. The proposed frequentist prediction intervals are publicly available from the R package `predint`, whereas R code for the computation of the two Bayesian prediction intervals is provided via GitHub.

Keywords: Bootstrap-calibration, micro-nucleus-test, long-term carcinogenicity studies, OECD test guideline, Shewhart control chart, Bayesian hierarchical modeling

1 Introduction

For several toxicological and pre-clinical study types it is mandatory to store and report the outcome of the negative and sometimes also positive control groups of the experiments conducted before the current study (see e.g. OECD guidelines 471, 487, 489 or EFSA 2024). In this context it is required to validate the concurrent control group by so called historical control limits (HCL) which, based on the HCD aim to predict the outcome of the current control group with x % (usually 95 %) of confidence (Kluxen et al. 2021, Dertinger et al. 2023, Menssen 2023).

This approach is seen as a quality check for the current control group(s) and it is interpreted as a warning signal, if the current control is not covered by the HCL (Vandenberg et al. 2020): Either as a warning for a false-positive result of the current study (if the concurrent control falls below the lower HCL) or as a warning for a false-negative result (if the concurrent control falls above the upper HCL). With other words, it is desired that the HCL cover the central 95 % of the possible values that can be obtained from the true underlying distribution. Despite the fact, that the HCL based validation of a current control is required by several test guidelines (e.g. OECD 471, OECD 473, OECD 487, OECD 490), most guidelines fail to provide reproducible methodology on how to compute HCL. Hence, many heuristics such as the historical range (the min and the max of the HCD) or the mean ± 2 standard deviations are used for the practical calculation of HCL, but suffer from severe theoretical drawbacks (Menssen 2023). However, this problem can be overcome by the application of prediction intervals, which, based on historical observations (the HCD) directly aim to predict one (or more) value(s) which are derived from the same data generating process (the current control group). Hence several authors recommend the use of prediction intervals for the application of HCL (EFSA 2024, Menssen and Schaarschmidt 2019, Menssen and Schaarschmidt 2022, Menssen 2023, Kluxen et al. 2021, Dertinger et al. 2023).

However, for the proper application of prediction intervals, it is crucial to account for the hierarchical design of the historical control data: Due to the fact that certain experimental units belong to a certain control group (blue panels in fig 1), HCD is comprised of at least one level of hierarchy. Sometimes it might happen, that further levels of hierarchy are present

within each control (or treatment) group e.g. that certain animals within a control group belong to a certain cage (shape of the dots in 1). Since each trial is comprised of different living experimental units (cells or animals) standardization between the trials (with respect to the experimental units) is only possible up to a certain extent. Furthermore, lab personnel, housing conditions or animal (or cell) suppliers might change between different historical studies.

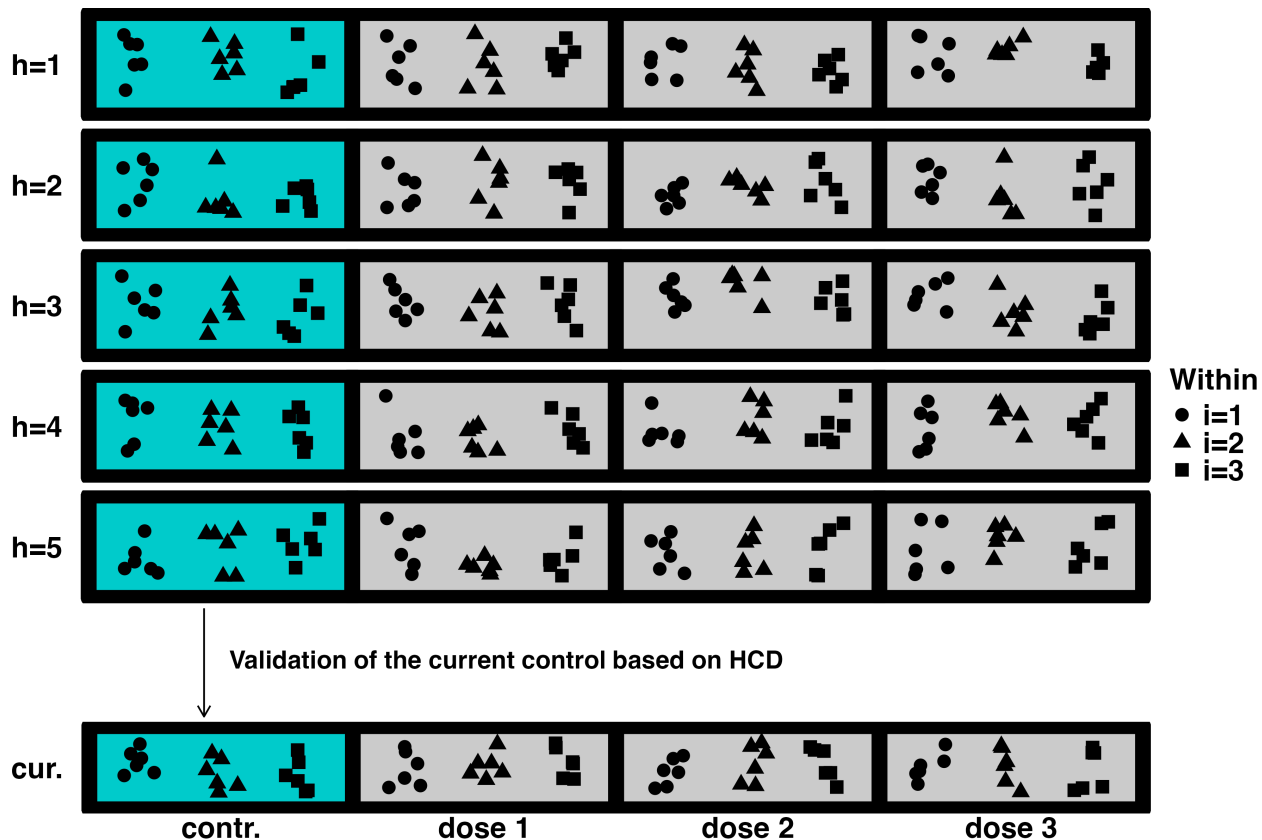


Figure 1: Scheme of the hierarchical design of toxicological HCD and the current trial. **Blue panels:** Control groups of different toxicological studies. **Grey panels:** Treatment groups of the different toxicological studies, which are usually not taken into account for HCD applications. **Black dots:** Individual experimental units. **Shape of the dots:** Possible within group randomization.

The fact that different experimental units belong to different control groups gives rise to systematic between study variation, which usually reflects both: Controllable causes (e.g. differences in handling of experimental units) as well as uncontrollable causes (e.g. the

biological variation within the population of the experimental units). This means, that the sheer presence of systematic between study variation is not problematic, but it is rather its magnitude that has to be considered (Deringer et al. 2023). However, this matter needs assay specific discussions by the toxicological community which are off-topic of this manuscript.

It has to be noted that the prediction intervals presented in several standard textbooks and other scientific publications (e.g. Hahn and Meeker 1991, Hahn et al. 2017, Wang 2008, Tian et al. 2022, Nelson 1982) ground on the assumption that the historical sample is unstructured and hence comprised of independent and identically distributed observations, meaning that between-study variability is assumed to be absent. As explained above, this assumption does not make sense in the context of toxicological HCD for which systematic between study variation is a fundamental part of the data generating process, and hence, is regularly reported in real life data. For example, HC data sets that are prone to systematic between study variation can be found in Tarone 1982, Carlus et al. 2013, Menssen et al. 2024, Levy et al. 2019, Tug et al. 2024, Dertinger et al. 2023 (for further details see section 4 of the supplementary material).

In toxicology several study types assess dichotomous endpoints: e.g. Carcinogenicity studies (rats with vs. rats without a tumor), the micro nucleus test (cells with vs. cells without a micronucleus) or the recently developed liquid microplate fluctuation Ames MPFTM test following Spiliotopoulos et al. 2024 (numbers of wells with vs. number of wells without a color change).

It seems natural to model such data based on the binomial distribution. But, as described before, the clustered nature of the HCD gives rise for systematic between-study variation. With other words, if systematic between-study variation is present, the variability of the data will exceed the variance that can be modeled by the simple binomial distribution. This effect is called overdispersion (or extra-binomial variation) and can either be modeled based on the quasi-binomial assumption - which relies on the assumption that the between study overdispersion is constant - or based on the beta-binomial distribution in which the between study overdispersion depends on the number of experimental units within each HC group (see section 2).

In the following, we provide four different methods to compute prediction intervals for

overdispersed binomial data: Two frequentist intervals that depend on normal approximation and bootstrap calibration as well as two Bayesian intervals of which one is based on Bayesian hierarchical modeling, whereas the other depends on the Bayesian version of a generalized linear random effects model.

The manuscript is organized as follows: The next section provides an overview about the modeling of overdispersed binomial endpoints. Section 3 provides an overview about the calculation of HCL. Several heuristical HCL that are used in daily toxicological routine are given in section 3.1. The proposed prediction intervals are described in sections 3.2 and 3.3. Section 4 reviews the properties of two real life HC data bases, that serve as an inspiration for Monte-Carlo simulations regarding the coverage probabilities of the proposed methodology (section 5). The application of the proposed methods is demonstrated in section 6. The manuscript ends with a discussion (section 7) and conclusions (section 8).

2 Models for overdispersed binomial data

2.1 Aggregated data

As described above (see fig. 1), HCD is comprised of $h = 1, \dots, H$ historical control groups but further levels of hierarchy can occur within each control group. For example, it is usual in rodent experiments, that within a certain control group, a predefined number of individuals n_{hi} are housed together in one of $i = 1, \dots, I$ cages. Nevertheless, it frequently happens in practice, that dichotomous HCD is documented aggregated on the level of the control groups (omitting the information about the randomization structure within each control group).

A prominent example for this way of reporting is the Historical Control Data Base of the U.S. National Toxicology Program (NTP 2024). In this data base, the total number of rats (or mice) with a certain tumor is presented on control group level (one value per control group) and the information how many rats were housed per cage is only available as meta-data that does not allow to track which rat (or mouse) belonged to a certain cage (as marked by the different shapes in fig. 1). Hence, the aggregation on control group level, leads to the loss of information on the randomization structure within a control group. Consequently, it is not

possible to account for potential within control group overdispersion (caused by systematic differences between cages). To account for this type of reporting, also the prediction intervals presented below are based on aggregated data.

If n_{hi} is the number of experimental units per within control group randomization unit (e.g. cages) and $y_{hi} \in \{0, 1, \dots, n_{hi}\}$ is the observed number of successes among them, aggregation on control group level yields

$$y_h = \sum_{i=1}^I y_{hi}$$

experimental units with a finding, out of

$$n_h = \sum_{i=1}^I n_{hi}$$

experimental units within the whole control group.

2.2 Modeling between-study overdispersion

One possible way to model overdispersion is the beta-binomial distribution in which the binomial proportion for each cluster is derived from a beta distribution

$$\pi_h \sim \text{Beta}(a, b) \tag{1}$$

and the random variable within each cluster is binomial

$$Y_h \sim \text{Bin}(n_h, \pi_h). \tag{2}$$

In this setting $E(\pi_h) = \pi = a/(a+b)$, $E(Y_h) = n_h\pi$, π is the overall binomial proportion and n_h is the a priori known and fixed total number of experimental units per historical control group. The variance of the beta-binomial distributed random variable is

$$\text{var}(Y_h) = n_h\pi(1 - \pi)[1 + (n_h - 1)\rho]. \tag{3}$$

In this parametrisation $\rho = 1/(1 + a + b)$ describes the intra-class correlation coefficient (Lui et al. 2000). Please note, that the parameters of the beta distribution are restricted to be $a > 0$ and $b > 0$. Hence also the intra-class correlation is restricted to be $\rho > 0$.

Another possibility to model between-study overdispersion is the quasi-binomial approach in which the dispersion parameter ϕ constantly inflates the variance

$$\text{var}(Y_h) = n_h \pi (1 - \pi) \phi. \quad (4)$$

Note, that in the case in which the number of experimental units within each control group becomes equal ($n_h = n_{h'}$) also the part of the beta-binomial variance that controls the magnitude of overdispersion per control group ($[1 + (n_h - 1)\rho]$ in eq. 3) becomes a constant. Consequently, in this special case, both models are not in contradiction to each other (Menssen and Schaarschmidt 2019) and

$$\phi \hat{=} [1 + (n_h - 1)\rho] \text{ if all } n_h = n_{h'}. \quad (5)$$

3 Historical control limits for overdispersed binomial data

The calculation of the historical control limits $[l, u]$ given below is based on the observed number of experimental units with an event y_h out of a total number of experimental units per historical control group n_h (e.g. rats with a tumor out of a total number of rats). All historical control limits (HCL) are aimed to cover a further number of experimental units with an observed number of successes $y^* = y_{H+1}$ out of a further a priori known total number of experimental units $n^* = n_{H+1}$ with coverage probability

$$P(l \leq y^* \leq u) = 1 - \alpha. \quad (6)$$

Since HCL are computed to validate the current control group, the desired HCL should aim to cover the central $100(1 - \alpha)\%$ of the underlying distribution and its limits should approach the lower $\alpha/2$ and the upper $1 - \alpha/2$ quantile, respectively (see fig. 1 of Francq et al. 2019). It is crucial to ensure for this behavior also if the underlying distribution is skewed (Hoffman 2003). Consequently, the desired interval has to ensure for equal tail probabilities

$$P(l \leq y^*) = P(y^* \leq u) = 1 - \alpha/2. \quad (7)$$

This means that the control limits practically cut off the lower and the upper $100(\alpha/2)\%$ of the underlying distribution, regardless if this distribution is symmetrical or skewed. For overdispersed binomial data, possible skewness depends on three factors:

1. The skewness increases, the closer π approaches its boundaries (0 or 1).
2. The skewness tends to increase with increasing between-study overdispersion (depending on the value for π).
3. The skewness also tends to increase with decreasing cluster size n^* (depending on the values for π and the amount of between-study overdispersion).

This behavior is demonstrated in fig. 1 and 2 of the supplementary material.

3.1 Heuristical historical control limits

Although several authors, dissuade from its use (Greim et al. 2003, Kluxen et al. 2021, EFSA 2024, Menssen 2023, Menssen et al. 2024), HCL based on the historical range are frequently applied in daily toxicological routine (Zarn et al. 2024, WHO 2023, NTP 2018, EFSA 2010). Since such HCL are given by

$$\left[l = \min(y_h), u = \max(y_h) \right] \quad (8)$$

they aim to cover *all* realizations from the underlying distribution and hence, do not aim for a proper approximation of its central $100(1 - \alpha)\%$ (but can be rather interpreted as a heuristical 100% prediction interval which does not provide practically useful control limits). Note that the min and max of the observed data provide very poor estimates for the true min and max of the underlying distribution, especially if the number of historical observations is low. This is because values in the center of the distribution have a higher chance to occur, whereas the occurrence of more extreme values in the tails of the distribution are less likely. Furthermore it has to be noted, that this interval is explicitly based on the assumption of constant cluster size $n_h = n^* \forall h = 1, \dots, H$, because the interpretation of the number of observed events makes only sense in relation to the given cluster size (meaning that 5 out of 50 rats with a tumor have a fundamental different interpretation than 5 out of 100 rats).

Hence, a sensible interpretation of the historical range is not possible, if the cluster size differs between the studies.

Another popular method for the calculation of control limits for dichotomous data are the limits used in Shewhart np-charts

$$[l, u] = n^* \bar{\pi} \pm k \sqrt{n^* \bar{\pi} (1 - \bar{\pi})} \quad (9)$$

with $\bar{\pi} = \frac{\sum_h y_h}{\sum_h n_h}$. In practical applications k is usually set to 2 or 3 in order to approximate the central 95.4 % or 99.7 % of the underlying distribution (Montgomery 2019). This HCL are strictly based on the assumption that the observations are independent realizations of the same binomial distribution which can be adequately approximated by a normal distribution with mean $n^* \bar{\pi}$ and variance $n^* \bar{\pi} (1 - \bar{\pi})$. Hence, the Shewhart np-chart presumes that the law of large numbers is applicable, ignores the variability in $\bar{\pi}$, fails to account for overdispersion and fails to ensure for equal tail probabilities.

HCL that are based on the mean $\pm k$ standard deviations are given by

$$[l, u] = \bar{y} \pm kSD \quad (10)$$

with $\bar{y} = \frac{\sum_h y_h}{H}$ and $SD = \sqrt{\frac{\sum_h (\bar{y} - y_h)^2}{H-1}}$. This type of HCL is based on a simple normal approximation that lacks an explicit assumption about the mean-variance relationship and hence heuristically allows for overdispersion (Menssen et al. 2024). Similar to HCL that are based on the historical range, the mean $\pm k$ standard deviations are explicitly based on the assumption of constant cluster size $n_h = n^* \quad \forall \quad h = 1, \dots, H$, because for dichotomous endpoints, the number of observed experimental units with an event is only interpretable in the context of the total number of experimental units in the particular control group. Hence, the application of HCL that are computed by the mean $\pm k$ standard deviations to dichotomous HCD with different sample sizes should strictly be avoided (see section 2 of the supplementary material).

3.2 Bootstrap calibrated prediction intervals

Similarly to the prediction intervals for overdispersed count data of Menssen et al. 2024, the two frequentist prediction intervals below are based on the assumption that

$$\frac{n^*\hat{\pi} - Y^*}{\sqrt{\text{var}(n^*\hat{\pi}) + \text{var}(Y^*)}} \overset{\text{approx.}}{\sim} N(0, 1).$$

Here, Y^* is the future random variable (of which y^* is a realization), $\hat{\pi}$ is the binomial proportion estimated from the HCD and n^* is the a priori known number of experimental units of the future control group and $n^*\hat{\pi}$ and Y^* are assumed to be independent random variables.

If between-study overdispersion is modeled based on the quasi-binomial assumption, the corresponding prediction interval is given by

$$[l, u] = n^*\hat{\pi} \pm z_{1-\alpha/2} \sqrt{\frac{\hat{\phi}n^{*2}\hat{\pi}(1-\hat{\pi})}{\sum_h n_h} + \hat{\phi}n^*\hat{\pi}(1-\hat{\pi})} \quad (11)$$

with $\hat{\phi} > 1$ as an estimate for the between-study overdispersion.

If between-study overdispersion is modeled based on the beta-binomial distribution, the corresponding prediction interval is given by

$$[l, u] = n^*\hat{\pi} \pm z_{1-\alpha/2} \sqrt{\left[\frac{n^{*2}\hat{\pi}(1-\hat{\pi})}{\sum_h n_h} + \frac{\sum_h n_h - 1}{\sum_h n_h} n^{*2}\hat{\pi}(1-\hat{\pi})\hat{\rho} \right] + n^*\hat{\pi}(1-\hat{\pi})[1 + (n^* - 1)\hat{\rho}]} \quad (12)$$

with $\hat{\rho}$ as an estimate for the intra-class correlation coefficient. Details on methodology for the estimation of $\hat{\pi}$, $\hat{\phi}$ and $\hat{\rho}$ are given in section 3.4).

As mentioned above, overdispersed binomial data can be heavily right- or left-skewed, but the prediction intervals in eq. 11 and 12 are still symmetrical. Furthermore, they depend on normal approximation and hence, tend to have coverage probabilities below the nominal level, especially if the number of historical studies is low.

To overcome this problem, a bootstrap calibration algorithm (see box below), that individually calibrates both interval borders was applied. Note, that the idea behind this algorithm is similar to a Monte-Carlo simulation regarding the prediction intervals coverage probability. Therefore, the bootstrap samples \mathbf{y}_b that mimic the HCD, as well the bootstrapped future

observation y_b^* are derived from the same data generating process (which depends on the estimates for the model-parameters estimated from the HCD). The algorithm aims to provide substitutes q_l and q_u for the standard normal quantile used in eq. 11 and 12, such that possible skewness of the underlying distribution is taken into account to ensure for equal tail probabilities and enhance the intervals coverage probability.

Bootstrap calibration of the proposed prediction intervals

1. Based on the historical data $\mathbf{y} = (y_1, \dots, y_H)$ find estimates for the model parameters ($\hat{\pi}$ and $\hat{\phi}$ in the quasi-binomial case and $\hat{\pi}$ and $\hat{\rho}$ in the beta-binomial case)
2. Based on these estimates, sample B parametric bootstrap samples \mathbf{y}_b following the same experimental design as the historical data (for sampling algorithms see section 3 of the supplementary material)
3. Draw B further bootstrap samples y_b^* that mimic the possible numbers of success in a future control group of size n^* (using the same sampling algorithms as in step 2)
4. Based on \mathbf{y}_b obtain bootstrapped estimates for the model parameters (either $\hat{\pi}_b$ and $\hat{\phi}_b$ or $\hat{\pi}_b$ and $\hat{\rho}_b$) and calculate $\widehat{var}_b(n^*\hat{\pi})$ and $\widehat{var}_b(Y^*)$
5. Calculate lower prediction borders $l_b = n^*\hat{\pi}_b - q_l\sqrt{\widehat{var}_b(n^*\hat{\pi}) + \widehat{var}_b(Y^*)}$, such that all l_b depend on the *same* value for q_l .
6. Calculate the bootstrapped coverage probability $\hat{\psi}_l = \frac{\sum_b I_b}{B}$ with $I_b = 1$ if $l_b \leq y_b^*$ and $I_b = 0$ if $y_b^* < l_b$
7. Alternate q_l until $\hat{\psi}_l \in (1 - \frac{\alpha}{2}) \pm t$ with t as a predefined tolerance around $1 - \frac{\alpha}{2}$
8. Repeat steps 5-7 for the upper prediction border with $\hat{\psi}_u = \frac{\sum_b I_b}{B}$ with $I_b = 1$ if $y_b^* \leq u_b$ and $I_b = 0$ if $u_b < y_b^*$

9. Use the corresponding coefficients q_l^{calib} and q_u^{calib} and the estimates obtained from the initial HCD (either $\hat{\pi}$ and $\hat{\phi}$ or $\hat{\pi}$ and $\hat{\rho}$) for interval calculation

$$\begin{aligned} l &= n^* \hat{\pi} - q_l^{calib} \sqrt{\widehat{var}(n^* \hat{\pi}) + \widehat{var}(Y^*)}, \\ u &= n^* \hat{\pi} + q_u^{calib} \sqrt{\widehat{var}(n^* \hat{\pi}) + \widehat{var}(Y^*)} \end{aligned}$$

The bootstrap calibrated quasi-binomial prediction interval is given by

$$\begin{aligned} l &= n^* \hat{\pi} - q_l^{calib} \sqrt{\frac{\hat{\phi} n^{*2} \hat{\pi} (1 - \hat{\pi})}{\sum_h n_h} + \hat{\phi} n^* \hat{\pi} (1 - \hat{\pi})} \\ u &= n^* \hat{\pi} + q_u^{calib} \sqrt{\frac{\hat{\phi} n^{*2} \hat{\pi} (1 - \hat{\pi})}{\sum_h n_h} + \hat{\phi} n^* \hat{\pi} (1 - \hat{\pi})}. \end{aligned} \tag{13}$$

Similarly, the bootstrap calibration of the beta-binomial prediction interval results in

$$\begin{aligned} l &= n^* \hat{\pi} - q_l^{calib} \sqrt{n^* \hat{\pi} (1 - \hat{\pi}) [1 + (n^* - 1) \hat{\rho}] + \left[\frac{n^{*2} \hat{\pi} (1 - \hat{\pi})}{\sum_h n_h} + \frac{\sum_h n_h - 1}{\sum_h n_h} n^{*2} \hat{\pi} (1 - \hat{\pi}) \hat{\rho} \right]} \\ u &= n^* \hat{\pi} + q_u^{calib} \sqrt{n^* \hat{\pi} (1 - \hat{\pi}) [1 + (n^* - 1) \hat{\rho}] + \left[\frac{n^{*2} \hat{\pi} (1 - \hat{\pi})}{\sum_h n_h} + \frac{\sum_h n_h - 1}{\sum_h n_h} n^{*2} \hat{\pi} (1 - \hat{\pi}) \hat{\rho} \right]}. \end{aligned} \tag{14}$$

The applied bootstrap calibration is a modified version of the algorithm proposed by Menssen and Schaarschmidt 2022 and has also been successfully applied to overdispersed count data (Menssen et al. 2024). The only difference to Menssen and Schaarschmidt 2022 is, that both interval limits are calibrated individually, but the search for q_l^{calib} and q_u^{calib} depends on the same bisection procedure using a tolerance $t = 0.001$.

Furthermore, the algorithm presented above differs from the calibration procedure used by Menssen and Schaarschmidt 2019 in two important aspects: First, contrary to Menssen and Schaarschmidt 2019 it calibrates both prediction borders separately and hence accounts for equal tail probabilities (see fig. 4 of the supplementary materials). Second, it aims to find substitutes for the complete standard normal quantile used for interval calculation, which in principal also enables simultaneous prediction of the outcome of more than one control group. This is possible if y_b^* is substituted by a bootstrap sample that mimics the outcome of several control (or treatment) groups.

3.3 Bayesian modeling

Bayesian approaches provide an alternative estimation of prediction intervals (Hamada et al. 2004). Future observations as well as all model parameters are interpreted as random variables depending on each other. Thus, a posterior distribution of a future observation can be derived immediately within the parameter estimation process.

3.3.1 Hierarchical modeling

Bayesian hierarchical modeling depends on the beta-binomial model that is given in equations 1 and 2. In a Bayesian interpretation, the experiments' parameters π_h are assumed to follow a Beta distribution, as a second level in a hierarchy (Howley and Gibbert 2003).

A Beta prior in mean-precision-parametrization (Beta proportion distribution, Stan development Team 2024a) is applied:

$$\pi_h \sim \text{Beta}(\mu, \kappa) \quad \forall h$$

with a non-informative prior for the location hyperparameter $\mu \in (0, 1)$. A weakly informative gamma prior $\kappa \sim \text{Ga}(a, b)$ should be applied to represent a realistic domain of the precision hyperparameter $\kappa > 0$ and, thus, to obtain a stable estimation.

The parameters' posterior distributions, given the data, i.e. symbolically

$$p(\pi_1, \dots, \pi_H, \mu, \kappa \mid Y_1, \dots, Y_H) \propto p(Y_1, \dots, Y_H \mid \pi_1, \dots, \pi_H) p(\pi_1, \dots, \pi_H \mid \mu, \kappa) p(\mu, \kappa) =$$

$$p(\mu, \kappa) \prod_{h=1}^H p(\pi_h \mid \mu, \kappa) p(Y_h \mid \pi_h)$$

are estimated by Markov-chain-Monte-Carlo (MCMC) sampling.

A posterior predictive distribution of a future observation y^* is obtained by random sampling per MCMC iteration $c = 1, \dots, C$: For every MCMC sample $(\tilde{\mu}_c, \tilde{\kappa}_c)$ of μ and κ , a prediction

$$\tilde{\pi}_c^* \sim \text{Beta}(\tilde{\mu}_c, \tilde{\kappa}_c)$$

of the future experiment's success proportion is drawn, and in turn a predicted future observation is sampled as

$$\tilde{y}_c^* \sim \text{Bin}(n^*, \tilde{\pi}_c^*).$$

A pointwise prediction interval for one future observation y^* is then obtained using empirical quantiles of $\{\tilde{y}_1^*, \dots, \tilde{y}_C^*\}$ such that

$$[l, u] = [q_{\alpha/2}(\{\tilde{y}_1^*, \dots, \tilde{y}_C^*\}), q_{1-\alpha/2}(\{\tilde{y}_1^*, \dots, \tilde{y}_C^*\})]$$

in the two-sided case.

3.3.2 Bayesian generalized linear mixed model

A concept closely related to the Beta-binomial model shown above is a generalized linear mixed model (GLMM), where Bernoulli distributed random variables Z_{h1}, \dots, Z_{hn_h} with $\sum_{k=1}^{n_h} Z_{hk} = Y_h$ are considered (Fong et al. 2010). The success proportion $\pi_h = E(Z_{hk})$ is linked to a linear predictor

$$\eta_h = \ln \frac{\pi_h}{1 - \pi_h} \in (-\infty, +\infty),$$

which is comprised of a fixed general intercept ν and random effects β_h per experiment:

$$\eta_h = \nu + \beta_h, \quad \beta_h \sim N(0, \sigma).$$

With that, the historical experiments are again assumed to have individual success proportions π_h , derived from the same distribution, and the observations are again realizations of the binomial random variable $Y_h \sim \text{Bin}(n, \pi_h)$.

The posterior distributions of $\nu \in (-\infty, +\infty)$ and $\sigma > 0$ are estimated by MCMC sampling using non-informative vague priors. Realizations of the future random variable $Y^* = \sum_{k=1}^{n^*} Z_k^*$ are derived: For every MCMC sample c , a prediction

$$\tilde{\beta}_c^* \sim N(0, \tilde{\sigma}_c)$$

of the future experiment's random intercept is drawn, followed by

$$\tilde{\eta}_c^* = \tilde{\nu}_c + \tilde{\beta}_c^*.$$

Then, the future experiment's success proportion

$$\tilde{\pi}_c^* = \frac{\exp(\tilde{\eta}_c^*)}{\exp(\tilde{\eta}_c^*) + 1}$$

is derived, and in turn

$$\tilde{y}_c^* \sim \text{Bin}(n^*, \tilde{\pi}_c^*)$$

is drawn from the latter. Similarly as above, a pointwise two-sided prediction interval for one future observation \tilde{y}^* is given by

$$[l, u] = [q_{\alpha/2}(\{\tilde{y}_1^*, \dots, \tilde{y}_C^*\}), q_{1-\alpha/2}(\{\tilde{y}_1^*, \dots, \tilde{y}_C^*\})].$$

3.4 Computational details and estimation

The proposed frequentist prediction intervals are implemented in the R package `predint` (Menssen 2023). The uncalibrated prediction intervals (eq. 11 and 12) are provided via `qb_pi()` and `bb_pi()`. The bootstrap calibrated prediction intervals (eq. 13 and 14) are implemented via the functions `quasi_bin_pi()` and `beta_bin_pi()`.

The estimates $\hat{\pi}$ and $\hat{\phi}$ used for the quasi-binomial prediction interval were estimated based on a generalized linear model (`stats::glm()`). The estimates $\hat{\pi}$ and $\hat{\rho}$ for the beta-binomial distribution were obtained following Lui et al. 2000. In order to avoid underspersion, the quasi-binomial interval was computed with $\hat{\phi} \geq 1.001$. The estimated intra-class correlation used for the beta-binomial interval was restricted to $\hat{\rho} \geq 0.00001$.

The bisection procedure used for bootstrap calibration is implemented in `predint` and provided via the function `bisection()`. This function takes three different lists as input, that contain the bootstrapped expected observations \hat{y}_b^* , the bootstrapped standard errors $\sqrt{\widehat{var}(n^*\hat{\pi})_b + \widehat{var}(Y^*)_b}$ and the bootstrapped further observations y_b^* and returns values for q_l and q_u . Hence, this function enables the calculation of bootstrap calibrated prediction intervals in a general way, such that any Wald-type prediction interval can be calibrated, as long as a parametric model can be fit to the data and a sampling function is available based on which parametric bootstrap samples can be generated.

The Bayesian hierarchical beta-binomial model was applied using the software `stan` via the R package `rstan` (Stan Development Team 2024). In the simulation, a weakly informative prior $\kappa \sim \text{Ga}(2, 5 \cdot 10^{-5})$ was used, giving the domain of the precision hyperparameter $\kappa > 0$. The Bayesian GLMM was applied using the R function `stan_glmmer` from the package `rstanarm` (Goodrich et al. 2024). Functions for the computation of both Bayesian prediction intervals

are provided via GitHub https://github.com/MaxMenssen/pi_overdisp_binomial/tree/main.

4 Properties of real life HCD

This section reviews the statistical properties of two real life HC data bases: One about long-term carcinogenicity studies and one about the micronucleus test. The properties of the two data bases were taken into account for the setup of the Monte-Carlo simulations regarding the coverage probability of the different HCL. This two study types were chosen in order to reflect the different properties of overdispersed binomial data at very different locations in the possible parameter space in order to enhance the simulations generalizability.

4.1 HCD from the micro-nucleus test

A micronucleus is a small fragment of chromosomes remaining outside the new nuclei after cell division. In the in-vitro micro-nucleus test (MNT), cell cultures on a well plate are treated with the compound of interest and an increased number of cells with a micronucleus is used as a proxy for genotoxicity (Fenech 2000). Negative and positive control wells are observed to measure the spontaneous micronucleus proportion without treatment and to evaluate the test assay's functionality by comparison to HCD.

The analyzed real life HCD includes negative and positive control groups from about $H \approx 50$ experiments. Due to the high extend of standardization, the aggregated number of scored cells per control group is always $n_h = n^* = 18000$.

The HC data base hints at an average proportion of cells with at least one micronucleus of about $\hat{\pi} \approx 0.01$ for negative control groups and about $\hat{\pi} \approx 0.15$ to 0.2 for positive controls. Overdispersion was estimated to range between $\hat{\phi} \approx 10$ and 50 for negative controls and tends to reach several hundreds for positive controls.

4.2 HCD from long-term carcinogenicity studies

Historical control data on different endpoints obtained in long-term carcinogenicity studies (LTC) are publicly available via the Historical Control Database of the U.S. National Toxicology Program (NTP 2024). From this resource Menssen and Schaarschmidt 2019 extracted HCD about the numbers of B6C3F1 mice per control group that had a hemangioma, the numbers of mice that showed at least one malignant tumor as well as the numbers of mice that passed away before the end of the study. This data was analyzed with regard to the binomial proportion $\hat{\pi}$ and the amount of overdispersion $\hat{\phi}$.

For rare events (hemangioma) the reported proportion was relatively low (close to zero) and overdispersion was estimated to be absent in most of the cases. The proportion of animals with malignant tumors ranged between 0.2 and 0.8, whereas the estimated dispersion parameters raised up to roughly four, meaning that the particular data set is four times as variable than possible under simple binomial distribution. The reported mortality rates behaved in a similar fashion. All reported control groups were comprised of 50 animals.

5 Simulation study

In order to assess the coverage probabilities of the different methods for the calculation of HCL reviewed above, Monte-Carlo simulations were run. In all simulations, the nominal coverage probability was set to $1 - \alpha = 0.95$. The parameter combinations used for the simulation were inspired by the real life data shown above. For all simulations the cluster size was fixed ($n_h = n^* \quad \forall \quad h = 1, \dots, H$) such that the variance-mean relationships of the beta-binomial distribution and the quasi-binomial assumption are not in contradiction to each other.

For each combination of model parameters, $S = 5000$ "historical" data sets were drawn, based on which historical control limits $[l, u]_s$ were calculated. Furthermore, S sets of single "future" observations y_s^* were sampled and the coverage probability of the control intervals

was computed to be

$$\hat{\psi}^{cp} = \frac{\sum_{s=1}^S I_s}{S} \text{ with}$$

$$I_s = 1 \text{ if } y_s^* \in [l, u]_s,$$

$$I_s = 0 \text{ if } y_s^* \notin [l, u]_s.$$

Furthermore, the ability of the different historical control limits to ensure for equal tail probabilities was checked. For this purpose the coverage of the simulated lower borders l_s and upper borders u_s was calculated additionally to the coverage probability for the whole interval. This was done as follows:

$$\hat{\psi}^l = \frac{\sum_{s=1}^S I_s}{S} \text{ with}$$

$$I_s = 1 \text{ if } l_s \leq y_s^*,$$

$$I_s = 0 \text{ if } l_s > y_s^*.$$

and

$$\hat{\psi}^u = \frac{\sum_{s=1}^S I_s}{S} \text{ with} \tag{15}$$

$$I_s = 1 \text{ if } y_s^* \leq u_s,$$

$$I_s = 0 \text{ if } u_s > y_s^*.$$

Average interval borders were calculated as the mean of the simulated interval borders

$$\bar{l} = \frac{\sum_{s=1}^S l_s}{S},$$

$$\bar{u} = \frac{\sum_{s=1}^S u_s}{S}.$$

Each single bootstrap calibrated prediction interval that was calculated in the simulation was based on $B = 10000$ bootstrap samples. Each Bayesian prediction interval was calculated based on $C = 5000$ MCMC samples.

5.1 Coverage probabilities for the MNT-inspired simulation setting

This part of the simulation was inspired by the properties of the real live HCD for the micro-nucleus test reviewed above. 72 combinations of values for the number of historical

studies H , the binomial proportion π and the amount of overdispersion ϕ were run, of which 18 combinations directly reflect the properties of the real life HCD (combinations of the bold faced parameter values in tab. 1), whereas the remaining 54 combinations of parameter values were run in order to enhance the generalisability of the simulation.

Note that, because the cluster size was relatively huge ($n_h = n^* = 18000$) most parameter combinations result in a relatively symmetrical underlying distribution (except for small proportions $\pi = 0.001$ combined with high overdispersion $\phi = 500$, see supplementary fig. 1).

Table 1: Parameter values used for the MNT-inspired simulation

Parameter	Values ¹
No. of historical studies (H)	5 , 10 , 20 , 100
Binomial proportion (π)	0.001, 0.01 , 0.1
Overdispersion (ϕ) ²	1.001, 3, 5, 10 , 50 , 500
Historical cluster size (n_h)	18000
Future cluster size (n^*)	18000

Bold numbers: Parameter values that reflect estimates obtained from real life HCD. **1:** Simulations were run for all 72 combinations of the given parameter values. **2:** Since the cluster sizes n_h and n^* are constant $\phi \hat{=} 1 + (n_h - 1)\rho \hat{=} 1 + (n^* - 1)\rho$. The given values of ϕ correspond to intra-class correlation coefficients ρ of 5.5e-08, 0.00011, 0.00022, 0.00050, 0.00272, 0.02772.

The simulated coverage probabilities of the heuristical methods are depicted in fig. 2, whereas the coverage probabilities of the proposed prediction intervals are presented in fig. 3. Furthermore, simulated average interval borders and the corresponding true quantiles are given in fig. 4 for three simulation settings, that reflect different levels of possible skewness of the underlying distribution. In these simulation settings H was set to 100 historical control groups. Thus, the historical information is high enough, that obvious flaws of the methods should be clearly visible and not be caused by too low historical sample size. None of the heuristics control the central 95 % of the underlying distribution, whereas all prediction intervals properly converge to the true quantiles, regardless if the underlying distribution is skewed or not.

As expected, the historical range (fig. 2A) covers the simulated future observations y_s^* in

all the cases, if the amount of historical control groups is high enough and lacks a proper control of the statistical error (here 5 %).

If overdispersion is practically absent ($\phi = 1.001$), the control limits of the np-chart (fig. 2B) yield coverage probabilities relatively close to the nominal level. But, with increasing overdispersion, their coverage probabilities decrease below 0.2, meaning that, by far, less than the desired central 95 % of the underlying distribution are covered. This is also demonstrated in fig. 4: The average limits of the np-chart are covered by the true quantiles. Consequently, the np-chart can not be recommended for the application to toxicological (overdispersed) HCD.

At first glance, it seems that the HCL computed by the mean ± 2 SD (fig. 2C) yield coverage probabilities close to the nominal level of 0.95, if the amount of historical control groups is high enough (at least 20). But, with a decreasing binomial proportion π and/or an increasing amount of overdispersion ϕ the right-skewness of the data increases. Hence, in many cases the lower border almost always covers the future observation (the triangles in fig. 2C approach 1) whereas the coverage probability of the upper border (crosses) does not approach the desired 0.975. This behavior demonstrates that HCL computed based on the mean ± 2 SD do not ensure for equal tail probabilities, or in other words: They do not control the central 95 % of the underlying distribution, if this distribution is skewed. This behavior is also demonstrated in fig. 4: The simulated average limits are systematically below the corresponding true quantiles, if the underlying distribution is right-skewed.

The coverage probabilities of the prediction intervals proposed in sections 3.2 and 3.3 are depicted in Figure 3. In general, both frequentist prediction intervals and the interval based on a Bayesian GLMM yield coverage probabilities relatively close to the nominal level for most settings. All three intervals behave in a comparable fashion, except for settings in which the number of historical control groups is low and / or the amount of overdispersion is high ($H < 10$, $\phi = 500$). Contrary to this, the prediction interval drawn from a Bayesian hierarchical model, fails to control the statistical error in many of the cases. Furthermore, Bayesian hierarchical models faced serious convergence issues, if the amount of historical studies and the amount of overdispersion was high ($H = 100$, $\phi = 500$), meaning that the desired interval could not be derived for many of the simulated data sets. Consequently, the

coverage probability could not be computed in this three cases (which explains the missing dots for $H = 100$ and $\phi = 500$ in 3D).

In the (practical) absence of overdispersion ($\phi = 1.01$), the beta-binomial prediction interval controls the alpha error best, whereas the prediction intervals based on the quasi-binomial assumption or a Bayesian GLMM tend to behave conservatively. But, in the absence of overdispersion, both intervals approach the nominal coverage probability with an increase of historical control groups. Contrary to this, the prediction interval obtained from Bayesian hierarchical modeling remains conservative in this setting, even for 100 historical studies.

For low to moderate proportions $\pi \in [0.001, 0.1]$ and low to moderate overdispersion $\phi \in [3, 50]$ (moderate in the context of $n_h = n^* = 18000$), all intervals, except the one based on Bayesian hierarchical modeling, yield coverage probabilities close to the nominal 0.95. The interval obtained from Bayesian hierarchical modeling approaches the nominal level only for 100 historical studies and remains liberal for a lower amount of historical information.

The right-skewness of the underlying distribution increases with a decreasing binomial proportion and an increasing amount of overdispersion (panels in the lower left of each sub-graphic). In this case, the sampled data contains many zeros and hence, the computed lower borders tend to always cover the future observation (the triangles approach 1). Hence, the prediction intervals practically aim to yield 97.5 % upper prediction borders. This effect is also visible in fig. 4 and reflects a core feature of the underlying distribution, rather than being based on model misspecification.

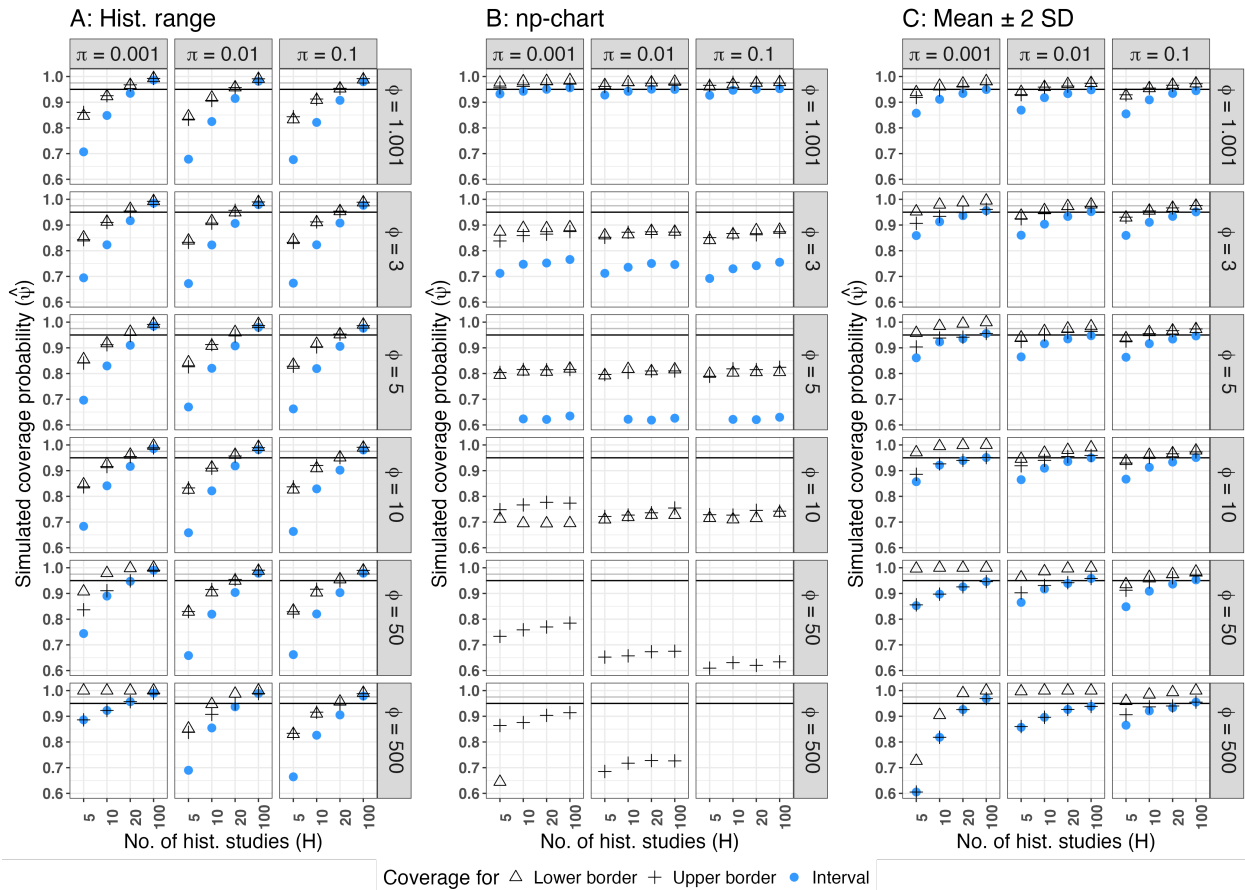


Figure 2: Simulated coverage probabilities of heuristical methods (MNT-setting). **A:** Historical range, **B:** np-chart, **C:** Mean \pm 2 SD, **Black horizontal line:** Nominal coverage probability $\psi^{cp} = 0.95$, **Grey horizontal line:** Nominal coverage probability for the lower and the upper limit, if equal tail probabilities are achieved $\psi^l = \psi^u = 0.975$. Coverage probabilities below 0.6 are excluded from the graphic.

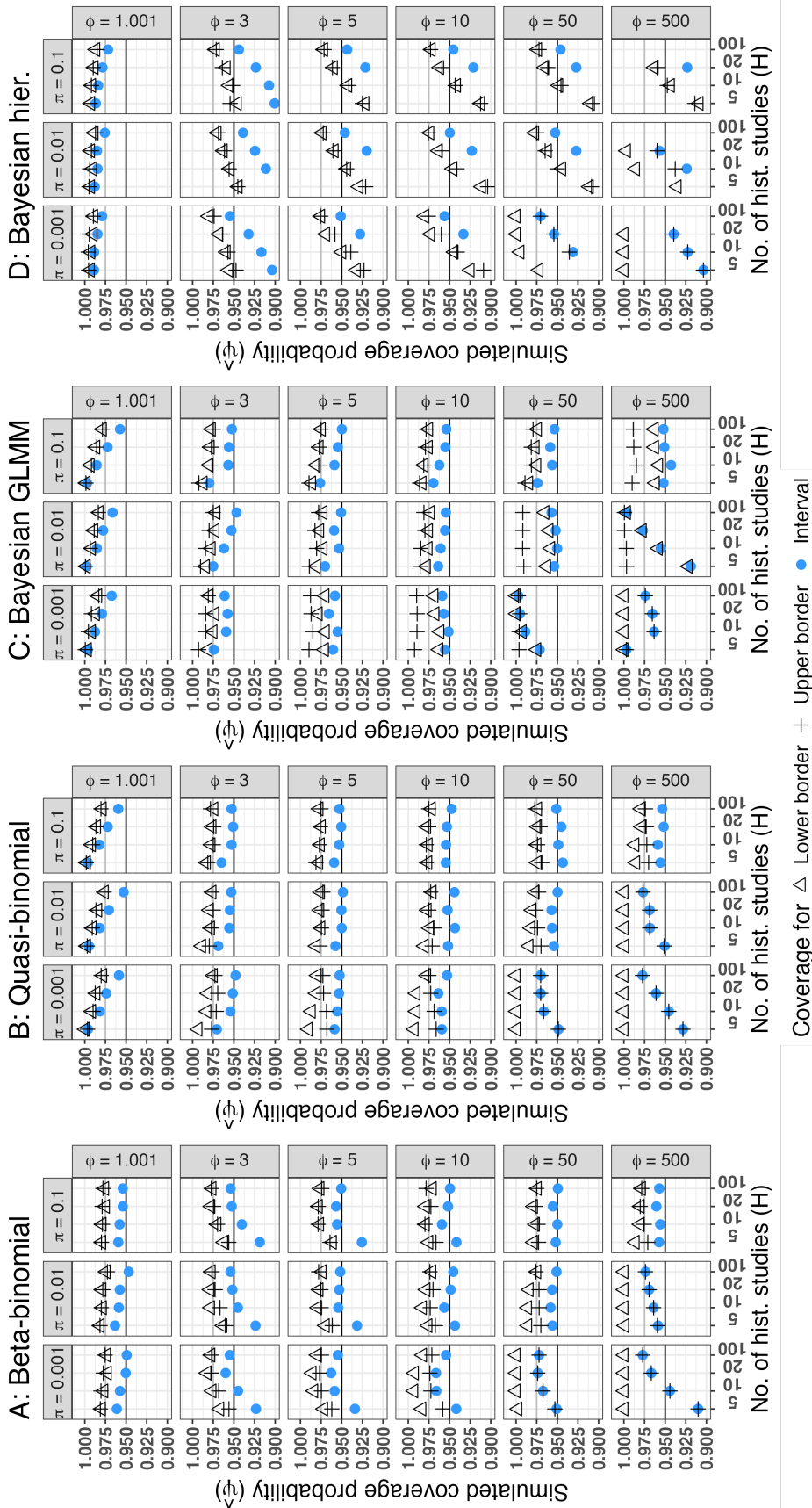


Figure 3: Simulated coverage probabilities of prediction intervals (MNT-setting). **A:** Calibrated beta-binomial prediction interval, **B:** Calibrated quasi-binomial prediction interval, **C:** Prediction interval obtained from a Bayesian generalized linear mixed model, **D:** Prediction interval obtained from a Bayesian hierarchical model, **Black horizontal line:** Nominal coverage probability $\psi^{cp} = 0.95$, **Grey horizontal line:** Nominal coverage probability for the lower and the upper limit, if equal tail probabilities are achieved $\psi^l = \psi^u = 0.975$. Coverage probabilities below 0.9 are not shown. The Bayesian hierarchical model faced serious convergence problems for $\phi = 500$ and $H = 100$. Hence, coverage probabilities could not be computed in this setting.

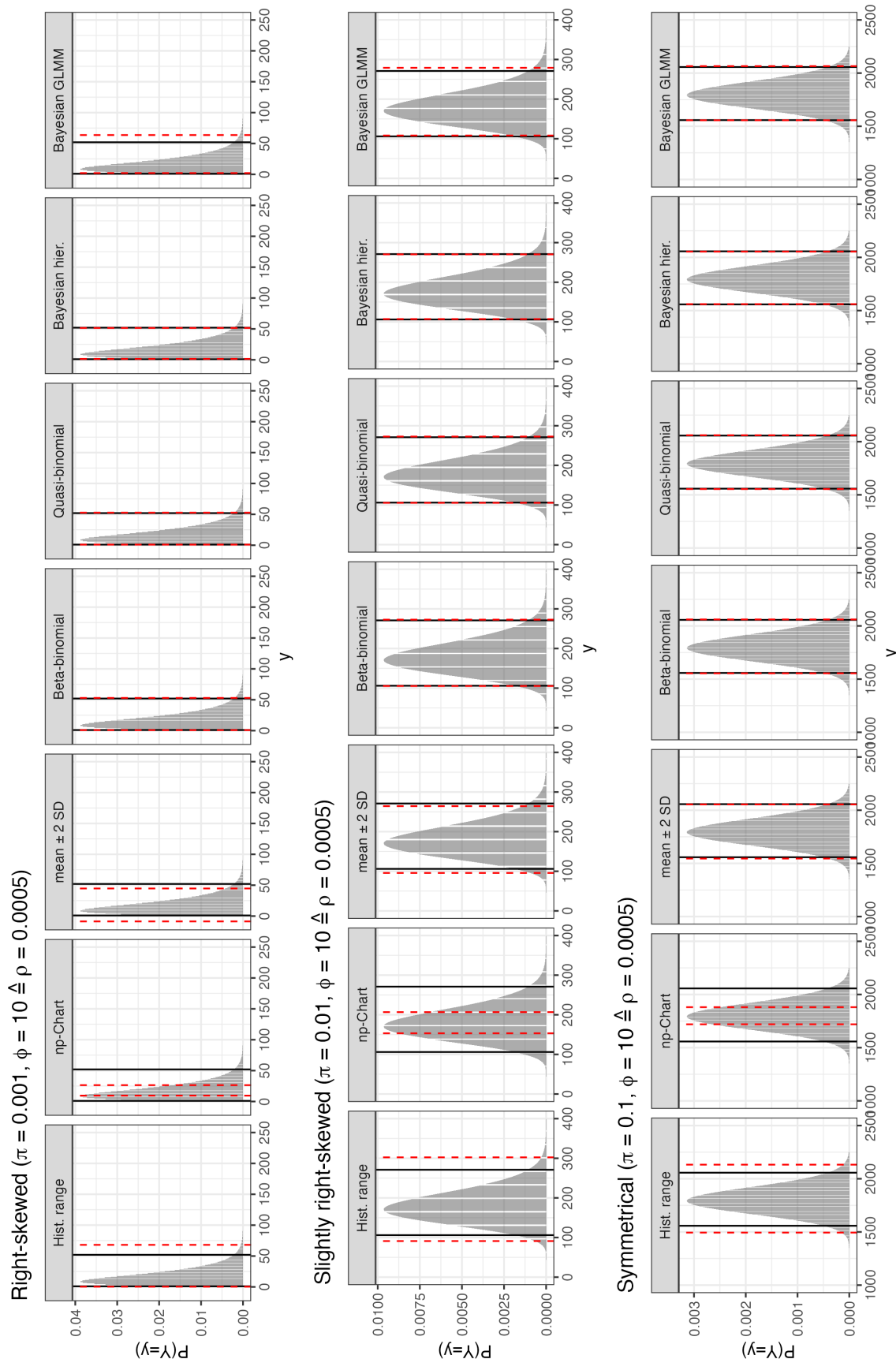


Figure 4: Average limits vs. true quantiles of the underlying distribution (MNT-setting). **Grey area:** Probability mass function of the underlying beta binomial distribution. **Black lines:** True underlying 2.5 % and 97.5% quantiles. **Dashed red lines:** Average limits for $H = 100$ and $n_h = 18000$ obtained from the simulation.

5.2 Coverage probabilities for the simulation setting inspired by long term carcinogenicity studies

This part of the simulation was inspired by the estimates for the binomial proportion and overdispersion reported by Menssen and Schaarschmidt 2019 for HCD obtained from long term carcinogenicity (LTC) studies run with B6C3F1 mice. 96 combinations of values for the number of historical studies H , the binomial proportion π and the amount of overdispersion ϕ were run, of which 54 combinations directly reflect the properties of the reported real life HCD (combinations of the bold faced parameter values in tab. 2), whereas the remaining 42 combinations of parameter values were run in order to enhance the generalisability of the simulation.

Table 2: Parameter values used for the LTC-inspired simulation

Parameter	Values ¹
No. of historical studies (H)	5, 10, 20 , 100
Binomial proportion (π)	0.01, 0.1, 0.2, 0.3, 0.4, 0.5
Overdispersion (ϕ) ²	1.001, 1.5, 3, 5
Historical cluster size (n_h)	50
Future cluster size (n^*)	50

Bold numbers: Parameter values that reflect estimates obtained from real life HCD. **1:** Simulations were run for all 96 combinations of the given parameter values. **2:** Since the cluster sizes n_h and n_* are constant with $\phi \hat{=} 1 + (n_h - 1)\rho \hat{=} 1 + (n^* - 1)\rho$, the given values of ϕ correspond to intra-class correlation coefficients ρ of 2.04e-05, 0.01020, 0.04081, 0.08163.

Due to the relatively small cluster size, the underlying distribution is heavily discrete and can become heavily right skewed for small proportions and/or high overdispersion (see fig.7). Hence, it is possible that in some settings (especially $\pi = 0.01$) the data contains many zeros. If it happened that a sampled "historical" data set contained only zeros ($y_h = 0 \quad \forall \quad h = 1, \dots, H$), the first observation was set to $y_1 = 0.5$ and the corresponding cluster size was set to $n_1 = 49.5$ following Menssen and Schaarschmidt 2019. This procedure was applied to all frequentist methods (heuristics and prediction intervals) in order to enable the estimation process in this extreme settings, whereas otherwise, the estimates for the binomial proportion and overdispersion would become zero. For almost all simulation

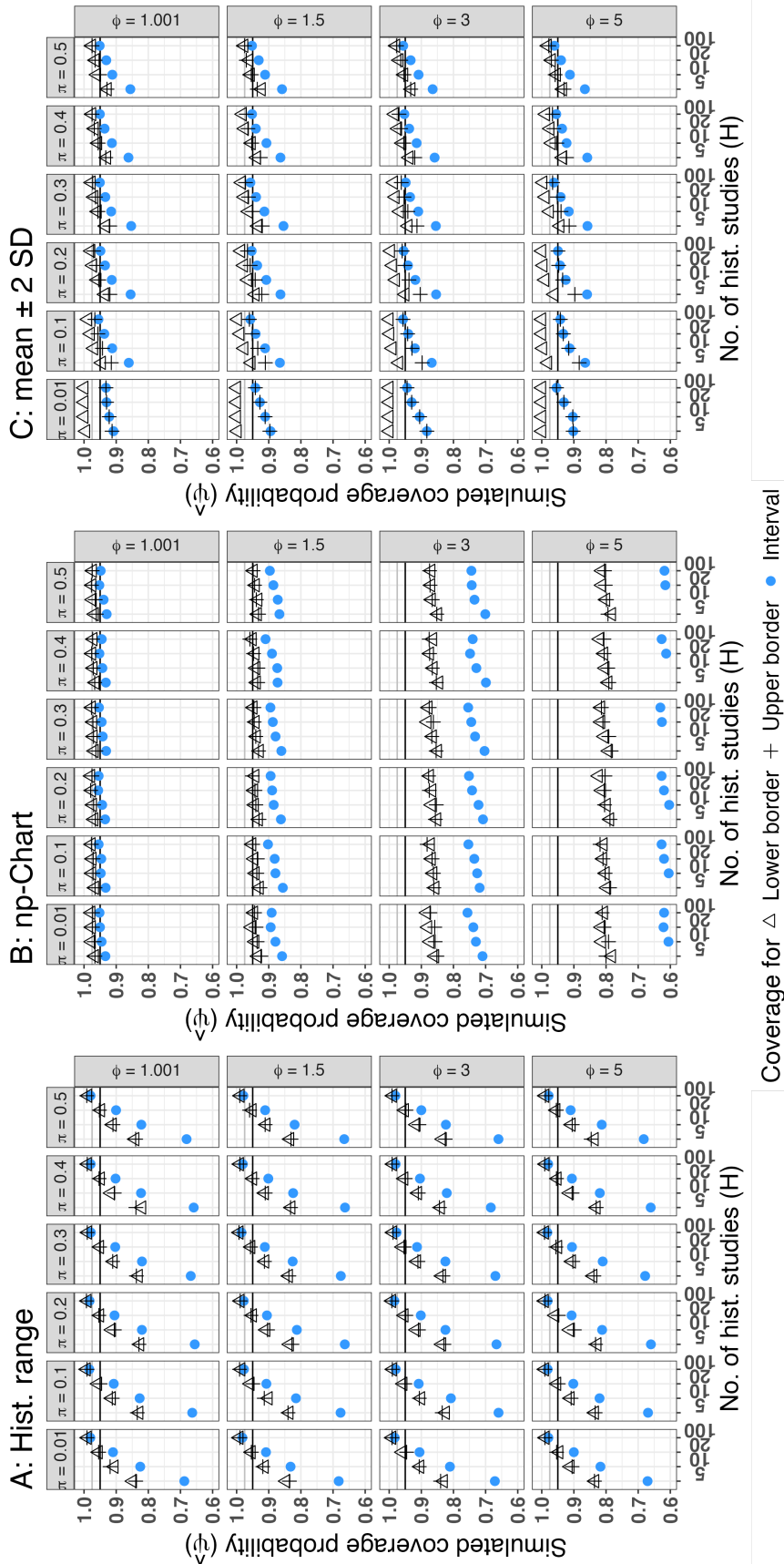


Figure 5: Simulated coverage probabilities of heuristical methods (LTC-setting) **A:** Historical range, **B:** np-chart, **C:** Mean \pm 2 SD, **Black horizontal line:** Nominal coverage probability $\psi^{\mathcal{P}} = 0.95$, **Grey horizontal line:** Nominal coverage probability for the lower and the upper limit, if equal tail probabilities are achieved $\psi^l = \psi^u = 0.975$. Coverage probabilities below 0.6 are excluded from the graphic

settings, Bayesian hierarchical modeling faced serious convergence problems. Therefore, the simulation results are heavily unreliable and not worth reporting. In particular, the precision hyperparameter related to overdispersion is very difficult to estimate, which also depends on the prior choice. Therefore, the only Bayesian method presented in this section is the prediction interval which is calculated based on a Bayesian GLMM.

The heuristical methods (Fig. 5) behaved in a similar fashion than in the MNT-setting: With rising amount of historical control groups, the future observation is always covered (Fig. 5A). In the absence of overdispersion, the np-Chart (Fig. 5B) yields coverage probabilities close to the nominal level, but with a rising amount of overdispersion, its coverage probabilities decrease below 0.6.

With a rising amount of historical control groups (at least 20), the coverage probabilities of the HCL computed by the mean ± 2 SD (Fig. 5C) approach the nominal level, if the underlying distribution is relatively symmetrical (low overdispersion and relatively high proportion). With increasing right-skewness of the underlying distribution (increasing overdispersion and decreasing proportion) and /or a low amount of historical control groups ($H < 20$) the HCL computed by the mean ± 2 SD yield coverage probabilities below the nominal level that can decrease to approximately 85 %.

In the practical absence of overdispersion ($\phi = 1.001$), the beta-binomial prediction interval (Fig. 6A) yields coverage probabilities satisfactorily close to the nominal 0.95 (except for $\pi = 0.01$), whereas the prediction intervals that are based on the quasi-binomial assumption (Fig. 6B) or drawn from a Bayesian GLMM (Fig. 6C) tend to remain conservative.

For $\pi \geq 0.2$, moderate overdispersion ($\phi \in [1.5, 3]$) and at least 10 historical control groups ($H \geq 10$) the coverage probabilities of the two frequentist prediction intervals satisfactorily approach the nominal 0.95, whereas the prediction interval obtained from the Bayesian GLMM remains slightly conservative, but may also be practically applicable in this scenario. Contrary, for high overdispersion ($\phi = 5$), the quasi-binomial and the Bayesian prediction interval yield coverage probabilities satisfactorily close to the nominal level (if $\pi \geq 0.2$ and $H \geq 10$). In this setting, the beta-binomial prediction interval yields coverage probabilities below the nominal level for $H = 5$ and remains conservative for $H = 10, 20$, but approaches the nominal level for $H = 100$.

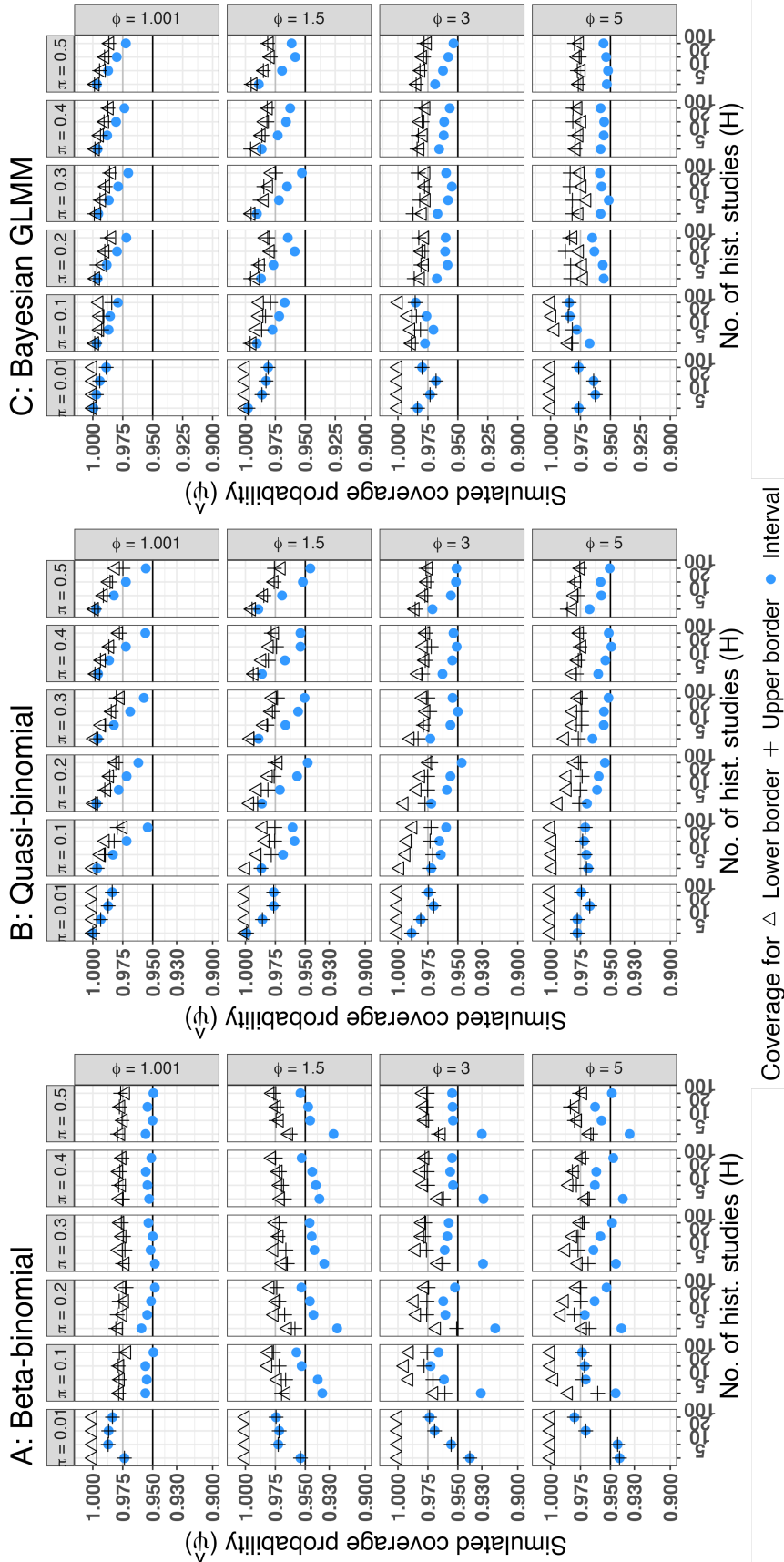


Figure 6: Simulated coverage probabilities of prediction intervals (LTC-setting) **A:** Calibrated beta-binomial prediction interval, **B:** Calibrated quasi-binomial prediction interval, **C:** Prediction interval obtained from a Bayesian GLMM, **Black horizontal line:** Nominal coverage probability $\psi^{cp} = 0.95$, **Grey horizontal line:** Nominal coverage probability for the lower and the upper limit, if equal tail probabilities are achieved $\psi^l = \psi^u = 0.975$.

With increasing overdispersion ϕ and decreasing proportions $\pi \leq 0.1$ the right skewness of the underlying distribution increases (see supplementary fig. 1 and 2) and its lower 2.5% quantile can approach zero (see fig. 7). With other words: in this case the lower prediction border aims to approximate a true quantile that is zero or close to zero.

This is the reason why all three prediction intervals practically yield 97.5 % upper prediction borders for $\pi = 0.01$ and the conservativeness of the lower borders increases for $\pi = 0.1$ with an increase of ϕ . This is not a misbehavior of the methodologies, but rather reflects a core feature of the underlying distribution and one should think about the application of an upper prediction border, rather than a prediction interval if many zeros are present in the data.

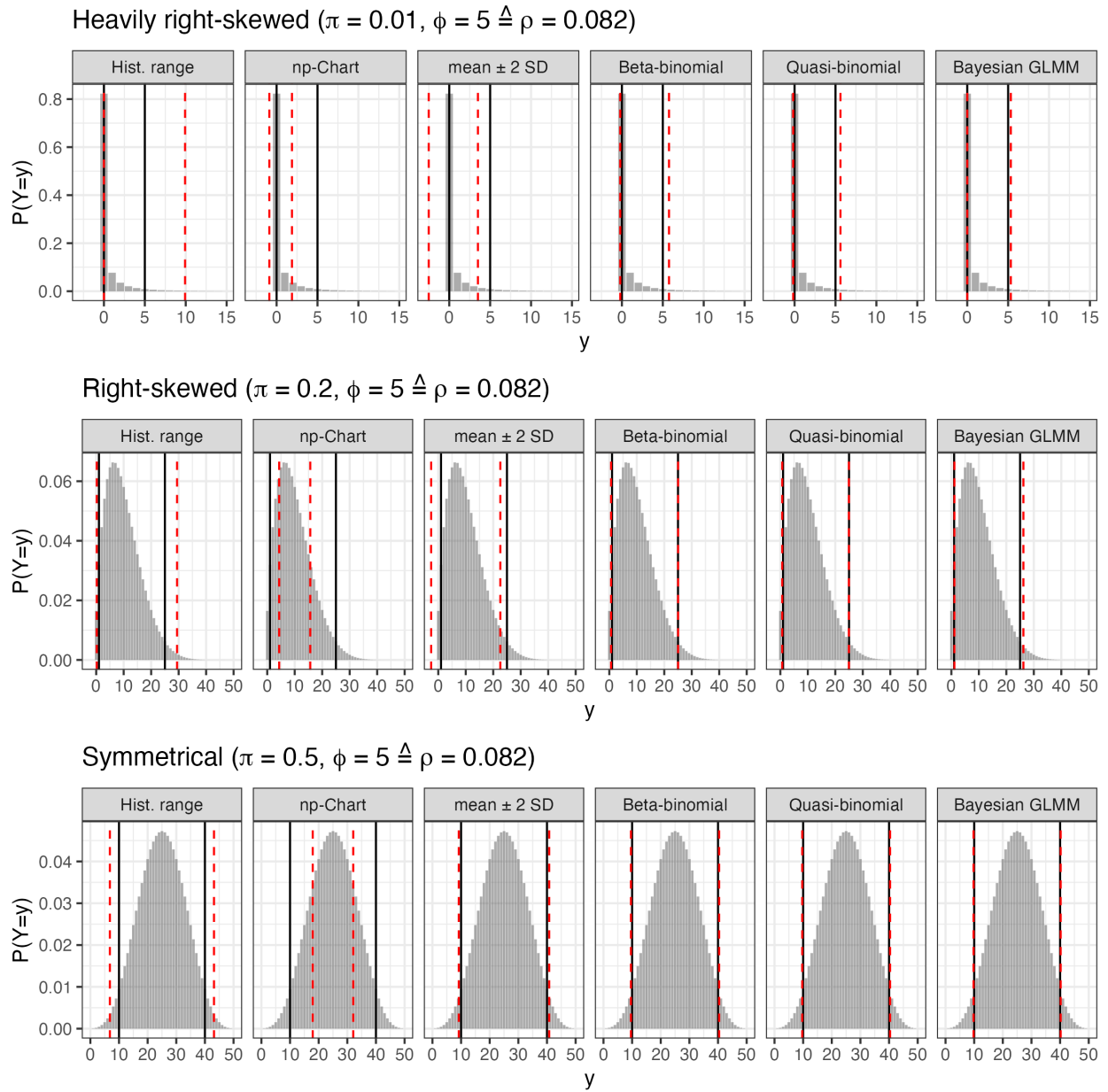


Figure 7: Average limits vs. true quantiles of the underlying distribution (LTC-setting). Grey area: Probability mass function of the underlying beta binomial distribution. Black lines: True underlying 2.5 % and 97.5% quantiles. Dashed red lines: Average limits obtained from the simulation.

6 Application of control limits

The calculation of HCL based on real life data is demonstrated using HCD about the mortality of male B6C3F1-mice in long-term carcinogenicity studies ($n_h = n^* = 50$). The data set was provided by Menssen and Schaarschmidt 2019 and contains negative controls from 10 different studies run between 2003 and 2011 on behalf of the NTP. It is available via the `predint` R package (Menssen 2024) under the name `mortality_HCD`.

The estimate for the binomial proportion is $\hat{\pi} = 0.276$ and slight overdispersion of $\hat{\phi} = 1.31$ appears to be present in the data (estimated with `stats::glm()`). The R code for the computation of the different HCL depicted in table 3 is available from GitHub (see link provided in section 3.4).

Table 3: Control limits (CL) for the mortality of male B6C3F1-mice obtained in negative controls of long term carcinogenicity studies at the National Toxicology Program.

Method	Lower CL	Upper CL	Interval width
Hist. range	10 (10)	21 (21)	11 (11)
np-chart	7.47 (8)	20.12 (20)	12.65 (12)
Mean \pm 2 SD	6.57 (7)	21.03 (21)	14.46 (14)
Beta-binomial ¹	6.33 (7)	22.24 (22)	15.91 (15)
Quasi-binomial (QP) ²	5.77 (6)	22.71 (22)	16.94 (16)
Bayesian hierarchical ³	7 (7)	21.025 (21)	14.025 (14)
Bayesian GLMM	6 (6)	23 (23)	17 (17)

Numbers in brackets: Lowest and highest number of events covered by the interval.

1: Estimates $\hat{\pi} = 0.276$ and $\hat{\rho} = 0.00621$ were obtained following Lui et al. 2000 (see computational details)

2: Estimates $\hat{\pi} = 0.276$ and $\hat{\phi} = 1.31$ were obtained based on `stats::glm` (see computational details)

3: A weakly informative prior $\kappa \sim \text{Ga}(2, 5 \cdot 10^{-3})$ was used.

The historical range yields the highest lower limit and the lowest upper limit and hence, the shortest control interval of all seven methods. Of the six methods that are aimed to cover a future observation with a probability of 0.95, the np-chart yields the shortest interval, because it does not account for the presence of overdispersion.

Practically, the mean \pm 2 SD and the prediction interval obtained from Bayesian hierarchical modeling yield the same limits [7, 21]. Both calibrated prediction intervals practically yield

upper limits of 22 but the lower limit of the quasi-binomial prediction interval is slightly lower than the beta-binomial one (6 vs. 7). With limits [6, 23], the prediction interval drawn from a Bayesian GLMM is the widest one and hence is in line with the simulation results that revealed a slightly conservative behaviour for a comparable LTC setting of $\phi = 1.5$, $H = 10$ and $\pi = 0.2$ (see Fig. 6C).

Note that, contrary to the description of the Bayesian hierarchical model given in section 3.4 (which basically aims at the MNT-inspired setting) a weakly informative prior $\kappa \sim \text{Ga}(2, 5 \cdot 10^{-3})$ was used for the precision hyperparameter κ . This adaption was necessary to reach convergence of the model.

7 Discussion

The validation of a concurrent control group based on prediction intervals is recommended by several authors (Menssen 2023, Kluxen et al. 2021) and since shortly, seems to be preferred by the European Food Safety Agency (EFSA 2024) over other (heuristic) methods. Nevertheless, since literature for the calculation of prediction intervals for clustered dichotomous data is relatively scarce, the practical application of HCL tends to rely on several heuristics, such as the application of the mean ± 2 SD (Rotolo et al. 2021, Prato et al. 2023, de Kort et al. 2020, Kluxen et al. 2021) or limits from Shewhart control charts (Lovell et al. 2018, Dertinger et al. 2023). Our simulations have shown that heuristic methods do not control the statistical error to a satisfactory level and hence, can not be recommended for the practical validation of a current control group.

Contrary to this, we could show, that prediction intervals satisfactorily control the statistical error, if calculated based on a model that match the statistical properties of the HCD. Several prediction intervals are available from the literature that are based on the assumption of independent binomial distributed observations (see e.g. Meeker et al. 2017 or Wang 2008), but ignore the clustered structure of the HCD (and hence the possibility for between-study overdispersion). In the context of HCD from long term carcinogenicity studies, Menssen and Schaarschmidt 2019 showed, that these intervals fail to approach the nominal coverage probability in the presence of overdispersion. This demonstrates that between-study overdispersion

is a crucial part of the underlying data generating process and hence needs to be considered for HCL calculation.

The magnitude of overdispersion reflects the between-study variation which is commonly present in toxicological HCD and hence, can be found in several published HC data sets in the literature (Tarone 1982a, Tarone 1982b, Levy et al. 2019, Menssen et al. 2024, Carlus et al. 2013, Dertinger et al. 2023, Tug et al. 2024, see supplementary materials section 4). However, in practice, systematic between-study variation might be induced by a mixture of both, controllable causes such as different handling of experimental units by different lab personnel, as well as uncontrollable causes such as the genetic variation inherent in the population of experimental units. This means that in practice, overdispersed HCD should be handled with care in a way that the magnitude of overdispersion reflects mainly the biological variability that is inherent of the biological process under observation, rather than the variability that is induced by controllable causes.

Both of the calibrated prediction intervals are improved versions of the quasi-binomial prediction interval of Menssen and Schaarschmidt 2019 which rely on a bootstrap procedure that adapts the formerly symmetrical prediction interval to possible skewness of the underlying distribution. Note, that this bootstrap calibration procedure has already been applied successfully for the calculation of prediction intervals drawn from random effects models (Menssen and Schaarschmidt 2022) or for overdispersed count data (Menssen et al. 2024). This demonstrates that, as long as one is able to bootstrap new observations from a model and the prediction standard error $\sqrt{\widehat{var}(\hat{y}^*) + \widehat{var}(Y^*)}$ can be formulated, the presented bootstrap calibration procedure provides a standardized framework for the calculation of prediction intervals for various distributional assumptions and/or models. An implementation of the bisection used in step 8 and 9 of the bootstrap calibration is provided via the function `bisection()` of the R package `predint`.

The prediction intervals drawn from Bayesian hierarchical models yield coverage probabilities that mainly remain below the nominal level in the MNT-setting (if overdispersion is present), but the model did not converge to most of the simulated data sets that mimic HCD from carcinogenicity studies (mainly if many zeros were present in the data). It is noteworthy, that in the Monte-Carlo simulations, Bayesian hierarchical models were fit, always using the same

prior $\kappa \sim \text{Ga}(2, 5 \cdot 10^{-5})$ regardless of the simulation setting. But, from the application to the real life example it is obvious, that this type of model needs a case to case adaption of the prior distribution to provide a reasonable domain for the hyperparameter κ (which depends on the amount of overdispersion). This might, at least partly, explain the liberality of this method. Unfortunately, the necessity for a case by case adaption of the prior distribution is far beyond the scope of most practitioners who are in charge of the reporting of HCD (mainly toxicologists that are barely trained in statistics). Hence this necessity might be a drawback for practical application.

Contrary to the Bayesian hierarchical models, the Bayesian GLMM did not have convergence problems in the LTC-setting. But, the applied GLMM mainly yield prediction intervals with coverage probabilities above the nominal level (except for a higher amount of overdispersion). This is, because such models a priori assume overdispersion or, equivalently, additional non-zero between-study variability to be present, and hence provide estimates for the respective parameters, even if between-study variability is absent in the the data-generating process.

An alternative to a fully Bayesian approach might be the application of an empirical Bayes procedure in which the hyperparameters domain is pre-estimated from the HCD, similar to the approaches of Tarone 1982a who incorporated HCD in a trend test or Kitsche et al. 2012 who exploit HCD to be accounted for in a Dunnett-type mean comparison. Anyhow, to the authors knowledge, an empirical Bayes procedure for the calculation of prediction intervals for overdispersed binomial data does not exist and might be a subject for future research.

It is noteworthy, that the coverage probability of the calibrated intervals is mainly effected by the amount of available historical information, defined by the numbers of experimental units within each control group n_h and number of historical studies H . In most of the cases the amount of overdispersion or the magnitude of the binomial proportion is of minor importance (as long as one accepts that the lower border can become zero for low proportions and / or high overdispersion such that the desired 95 % prediction interval practically results in a 97.5 % upper prediction limit).

This means, that for a high cluster size (as in the MNT-setting) both calibrated prediction intervals yield coverage probabilities satisfactorily close to the nominal level even for only five historical control groups. Contrary, for smaller cluster sizes (as in the LTC-setting) the

number of historical control groups has to be slightly higher (say 10) to enable coverage probabilities close enough to the nominal level. Furthermore, note that with decreasing cluster size (n_h and n^*), the discreteness of the underlying distribution rises and hence, the nominal 0.95 coverage probability can not completely be achieved in all of the possible cases (Agresti 1998).

Since the bootstrap calibration procedure presented above has already been applied to enable the calculation of prediction intervals drawn from linear random effects models (Menssen and Schaarschmidt 2022) or in order to predict overdispersed count data (Menssen et al. 2024), it can be seen as a general and flexible tool for the calculation of prediction intervals. Hence, for the future it is planned to exploit its potential to enable the calculation for a broader range of models / distributions. Furthermore it is possible to extend the algorithm to enable the calculation of simultaneous prediction intervals, which also will be the subject of future research.

Another relevant application is the evaluation of HCD with individual (non-aggregated) values reported (e.g., for individual wells in one historical MNT-experiment rather than the complete plate), where extra-Binomial variability is also possible within one experiment (e.g. between the wells of the same plate). Here, GLMMs (both frequentist and Bayesian) as well as hierarchical models can be very helpful. Jeske and Young 2013 provided a bootstrap based procedure for the calculation of prediction intervals based on one-way GLMM, but to the authors knowledge, a general solution for the calculation of prediction intervals drawn from GLMM is not yet available. Hence, also this topic remains as an open issue that needs further investigation.

8 Conclusions

If overdispersion is present in the data (and its magnitude is tolerable):

- Commonly applied heuristics (e.g. hist. range, np-charts or mean \pm 2 SD) do not satisfactorily control the statistical error and hence, should not be applied for the calculation of HCL.
- Symmetrical HCL do not account for possible right- (or left-) skewness of the data and hence do not ensure for equal tail probabilities.
- In most of the cases, the bootstrap calibrated prediction intervals yield coverage probabilities closest to the nominal level and hence, outperform all other methods reviewed in this manuscript.
- Due to their poor statistical properties (coverage probabilities below the nominal level) and the need for a case to case adaption of prior distributions, prediction intervals drawn from Bayesian hierarchical models can not be recommended for practical application.
- Prediction intervals computed based on Bayesian GLMM have coverage probabilities which are relatively close to the nominal level (in most cases). Because they can be easily adapted to handle more than one level of hierarchy, they are promising candidates for the application to non-aggregated HCD.
- With an increasing amount of overdispersion and decreasing binomial proportion, the amount of zeros in the data increases. If the amount of zeros in the data is high enough, the lower border will always cover the future observation and consequently prediction intervals (Bayesian or frequentist) practically yield 97.5 % upper prediction limits. This behavior is not a drawback of the methodology, but rather reflects one of the core features of overdispersed binomial data.
- Software for the calculation of bootstrap calibrated prediction intervals is publicly available via the R package `predint`.

9 Acknowledgments

We have to thank Frank Schaarschmidt for fruitful discussions on prediction intervals and the impact of overdispersion on the inference drawn from dichotomous data. Furthermore, we have to thank both reviewers for their valuable comments which greatly helped to improve our manuscript.

10 References

Bain, L. J., Patel, J. K. (1993). Prediction intervals based on partial observations for some discrete distributions. *IEEE Transactions on Reliability*, 42(3), 459-463.

Bonapersona, V., Hoijtink, H., RELACS Consortium Abbinck M. 4 Baram TZ 5 6 Bolton JL 5 Bordes J. 7 Knop J. 1 Korosi A. 4 Krugers HJ 4 Li JT 8 9 Naninck EFG 4 Reemst K. 4 Ruigrok SR 4 Schmidt MV 7 Umeoka EHL 4 10 Walker CD 11 Wang XD 12 Yam KY 4, Sarabdjitsingh, R. A., Joëls, M. (2021). Increasing the statistical power of animal experiments with historical control data. *Nature neuroscience*, 24(4), 470-477.

Carlus, M., Elies, L., Fouque, M. C., Maliver, P., Schorsch, F. (2013). Historical control data of neoplastic lesions in the Wistar Hannover Rat among eight 2-year carcinogenicity studies. *Experimental and Toxicologic Pathology*, 65(3), 243-253.

de Kort, M., Weber, K., Wimmer, B., Wilutzky, K., Neuenhahn, P., Allingham, P., Leoni, A. L. (2020). Historical control data for hematology parameters obtained from toxicity studies performed on different Wistar rat strains: Acceptable value ranges, definition of severity degrees, and vehicle effects. *Toxicology Research and Application*, 4, 2397847320931484.

Demétrio, C. G., Hinde, J., Moral, R. A. (2014). Models for overdispersed data in entomology. *Ecological modelling applied to entomology*, 219-259.

Dertinger, S. D., Li, D., Beevers, C., Douglas, G. R., Heflich, R. H., Lovell, D. P., Roberts, D.J., Smith, R., Uno, Y., Williams, A., Witt, K.L., Zeller A., Zhou, C. (2023). Assessing the quality and making appropriate use of historical negative control data: A report of the International Workshop on Genotoxicity Testing (IWGT). Environmental and Molecular Mutagenesis.

EFSA (2010). Scientific Opinion on the re-evaluation of curcumin (E 100) as a food additive. EFSA J., 8, 1679.

EFSA (2024): Draft Scientific Opinion on the use and reporting of historical control data for regulatory studies. Public Consultation PC-0856. <https://connect.efsa.europa.eu/RM/s/consultations/publicconsultation2/a01Tk000000Cvs9/pc0856>

Fenech, M. (2000). The in vitro micronucleus technique. Mutation Research/Fundamental and Molecular Mechanisms of Mutagenesis, 455(1-2), 81-95.

Fong, Y., Rue, H., Wakefield, J. (2010). Bayesian inference for generalized linear mixed models. Biostatistics, 11(3), 397-412.

Francq, B. G., Lin, D., Hoyer, W. (2019). Confidence, prediction, and tolerance in linear mixed models. Statistics in medicine, 38(30), 5603-5622.

Gabry, J., Goodrich, B., Ali, I., Brillemann, S. (2024). Bayesian applied regression modeling via Stan. R Package rstanarm, version 2.32.1

Greim, H., Gelbke, H. P., Reuter, U., Thielmann, H. W., Edler, L. (2003). Evaluation of historical control data in carcinogenicity studies. Human & experimental toxicology, 22(10), 541-549.

Hamada, M., Johnson, V., Moore, L. M., Wendelberger, J. (2004). Bayesian prediction

intervals and their relationship to tolerance intervals. *Technometrics*, 46(4), 452-459.

Hoffman, D. (2003). Negative binomial control limits for count data with extra-Poisson variation. *Pharmaceutical Statistics: The Journal of Applied Statistics in the Pharmaceutical Industry*, 2(2), 127-132.

Howley, P. P., Gibberd, R. (2003). Using hierarchical models to analyse clinical indicators: a comparison of the gamma-Poisson and beta-binomial models. *International Journal for Quality in Health Care*, 15(4), 319-329.

Jeske, D. R., Yang, C. H. (2013). Approximate Prediction Intervals for Generalized Linear Mixed Models Having a Single Random Factor. *Statistics Research Letters*, 2(4), 85-95.

Kitsche, A., Hothorn, L. A., Schaarschmidt, F. (2012). The use of historical controls in estimating simultaneous confidence intervals for comparisons against a concurrent control. *Computational Statistics & Data Analysis*, 56(12), 3865-3875.

Kluxen, F. M., Weber, K., Strupp, C., Jensen, S. M., Hothorn, L. A., Garcin, J. C., Hofmann, T. (2021). Using historical control data in bioassays for regulatory toxicology. *Regulatory Toxicology and Pharmacology*, 125, 105024.

Krishnamoorthy K., and T. Mathew. (2009). *Statistical Tolerance Regions: Theory, Applications, and Computation*. John Wiley and Sons, Hoboken.

Krishnamoorthy, K., Peng, J. (2011). Improved closed-form prediction intervals for binomial and Poisson distributions. *Journal of Statistical Planning and Inference*, 141(5), 1709-1718.

Lovell, D. P., Fellows, M., Marchetti, F., Christiansen, J., Elhajouji, A., Hashimoto, K., Kasamotog, S., Lih, Y., Masayasui, O., Moorej, M.M., Schulerk, M., Smithl, R., Stankowski Jr.m,L.F., Tanakag, J., Tanirn, J.Y., Thybaudo, V., Van Goethemp F., Whitwell, J. (2018). Analysis of negative historical control group data from the in vitro micronucleus assay using

TK6 cells. *Mutation Research/Genetic Toxicology and Environmental Mutagenesis*, 825, 40-50.

Lui, K. J., Mayer, J. A., Eckhardt, L. (2000). Confidence intervals for the risk ratio under cluster sampling based on the beta-binomial model. *Statistics in medicine*, 19(21), 2933-2942.

Levy, D. D., Zeiger, E., Escobar, P. A., Hakura, A., Bas-Jan, M., Kato, M., Moore, M.M., Sugiyama, K. I. (2019). Recommended criteria for the evaluation of bacterial mutagenicity data (Ames test). *Mutation Research/Genetic Toxicology and Environmental Mutagenesis*, 848, 403074.

McCullagh P, Nelder J.A. (1989): *Generalized Linear Models*. 2nd Edition, Chapman and Hall, London.

Meeker, W. Q., Hahn, G. J., Escobar, L. A. (2017). *Statistical intervals: a guide for practitioners and researchers*. John Wiley & Sons.

Menssen, M., Schaarschmidt, F. (2019). Prediction intervals for overdispersed binomial data with application to historical controls. *Statistics in Medicine*, 38(14), 2652-2663.

Menssen, M., Schaarschmidt, F. (2022). Prediction intervals for all of M future observations based on linear random effects models. *Statistica Neerlandica*, 76(3), 283-308.

Menssen, M. (2023). The calculation of historical control limits in toxicology: Do's, don'ts and open issues from a statistical perspective. *Mutation Research/Genetic Toxicology and Environmental Mutagenesis*, 503695.

Menssen M. (2024). *predint: Prediction Intervals*. R package version 2.2.1

Menssen, M., Dammann, M., Fneish, F., Ellenberger, D., Schaarschmidt, F. (2024). Prediction

intervals for overdispersed Poisson data and their application in medical and pre-clinical quality control. *Pharmaceutical Statistics* (published online). <https://doi.org/10.1002/pst.2447>

Millard SP (2013). *EnvStats: An R Package for Environmental Statistics*. Springer, New York. ISBN 978-1-4614-8455-4

Montgomery, D. C. (2019). *Introduction to statistical quality control*. John Wiley & Sons.

Nelson, W. (1982). *Applied Life Data Analysis*. New York, NY: John Wiley & Sons.

NTP (2018): NTP Technical Report 595: Toxicology and Carcinogenesis Studies in Hsd:Sprague Dawley SD Rats Exposed to Whole-body Radio Frequency Radiation at a Frequency (900 MHz) and Modulations (GSM and CDMA) Used by Cell Phones. <https://ntp.niehs.nih.gov/publications/reports/tr/tr595>

NTP (2024): NTP Historical Controls Data Base. <https://ntp.niehs.nih.gov/data/controls>

OECD 471: Bacterial Reverse Mutation Test, OECD Guidelines for the Testing of Chemicals, Section 4, OECD Publishing, Paris.

OECD 473: In Vitro Mammalian Chromosomal Aberration Test, OECD Guidelines for the Testing of Chemicals, Section 4, OECD Publishing, Paris

OECD 487: In Vitro Mammalian Cell Micronucleus Test, OECD Guidelines for the Testing of Chemicals, Section 4, OECD Publishing, Paris.

OECD 489: In Vivo Mammalian Alkaline Comet Assay, OECD Guidelines for the Testing of Chemicals, Section 4, OECD Publishing, Paris.

OECD 490: In Vitro Mammalian Cell Gene Mutation Tests Using the Thymidine Kinase Gene, OECD Guidelines for the Testing of Chemicals, Section 4, OECD Publishing, Paris.

Prato, E., Biandolino, F., Parlapiano, I., Grattagliano, A., Rotolo, F., Buttino, I. (2023). Historical control data of ecotoxicological test with the copepod *Tigriopus fulvus*. *Chemistry and Ecology*, 39(8), 881-893.

Rotolo, F., Vitiello, V., Pellegrini, D., Carotenuto, Y., Buttino, I. (2021). Historical control data in ecotoxicology: Eight years of tests with the copepod *Acartia tonsa*. *Environmental Pollution*, 284, 117468.

Ryan, L. (1993). Using historical controls in the analysis of developmental toxicity data. *Biometrics*, 1126-1135.

Spiliotopoulos, D., Koelbert, C., Audebert, M., Barisch, I., Bellet, D., Constans, M., Czich, A., Finot, F., Gervais, V., Khoury, L., Kirchnawy, C., Kitamoto, S., Le Tesson, A., Malesic, L., Matsuyama, R., Mayrhofer, E., Mouche, I., Preikschat, B., Prielinger, L., Rainer, B., Roblin, C., Wäse, K. (2024). Assessment of the performance of the Ames MPF™ assay: A multicenter collaborative study with six coded chemicals. *Mutation Research/Genetic Toxicology and Environmental Mutagenesis*, 893, 503718.

Stan Development Team. (2024) RStan: the R interface to Stan. R package version 2.32.6.

Stan Development Team (2024). Stan functions reference. version 2.35.27

Tarone, R. E. (1982a). The use of historical control information in testing for a trend in proportions. *Biometrics*, 215-220.

Tarone, R. E. (1982b). The use of historical control information in testing for a trend in Poisson means. *Biometrics*, 457-462.

Tian, Q., Nordman, D. J., Meeker, W. Q. (2022). Methods to compute prediction intervals: A review and new results. *Statistical Science*, 37(4), 580-597.

Tug, T., Duda, J. C., Menssen, M., Bruce, S. W., Bringezu, F., Dammann, M., Frotschl, R., Harm, V., Ickstadt, K., Igl, B-W., Jarzombek, M., Kellner, R., Lott, J., Pfuhler, S., Plappert-Helbig, U., Rahnenfuhrer, J., Schulz, M., Vaas, L., Vasquez, M., Ziegler, V., Ziemann, C. (2024). In vivo alkaline comet assay: Statistical considerations on historical negative and positive control data. *Regulatory Toxicology and Pharmacology*, 148, 105583.

Valverde-Garcia, P., Springer, T., Kramer, V., Foudoulakis, M., Wheeler, J. R. (2018). An avian reproduction study historical control database: a tool for data interpretation. *Regulatory Toxicology and Pharmacology*, 92, 295-302.

Vandenberg, L. N., Prins, G. S., Patisaul, H. B., Zoeller, R. T. (2020). The use and misuse of historical controls in regulatory toxicology: lessons from the CLARITY-BPA study. *Endocrinology*, 161(5), bqz014.

Wang, H. (2008). Coverage probability of prediction intervals for discrete random variables. *Computational statistics and data analysis*, 53(1), 17-26.

Wang, H. (2010). Closed form prediction intervals applied for disease counts. *The American Statistician*, 64(3), 250-256.

WHO (2024). Pesticide residues in food 2022. Joint FAO/WHO meeting on pesticide residues. Evaluation Part II–Toxicological. World Health Organization.

Zarn, J. A., König, S. L., Shaw, H. V., Geiser, H. C. (2024). An analysis of the use of historical control data in the assessment of regulatory pesticide toxicity studies. *Regulatory Toxicology and Pharmacology*, 105724.

